Adsorption (2007) 13: 331–339
DOI 10.1007/s10450-007-9030-8

Fixed bed adsorption of benzothiophene over zeolites with faujasite structure

J.L. Sotelo · M.A. Uguina · V.I. Águeda

Received: 27 April 2007 / Revised: 19 July 2007 / Accepted: 23 July 2007 / Published online: 20 September 2007

Abstract This work addresses the adsorption of benzothiophene (BT), as a model heterocyclic and aromatic sulphur compound present in road fuels, over agglomerated zeolites with faujasite structure. Several adsorbents based on zeolites with FAU structure have been prepared with different Si/Al molar ratios and exchange cations and then agglomerated. The influence of the zeolite basicity has been studied, both in equilibrium and dynamic liquid phase adsorption experiments. Basicity of the adsorbent increased as the Si/Al molar ratio and the electronegativity of the exchange cation decreased. In equilibrium experiments, the affinity towards the adsorbent increased as the Si/Al molar ratio decreased, showing the highest affinity for exchanged low silica X zeolites with medium basicity (A-KLSX-02). Dynamic experiments showed that the less zeolite basicity, the higher fractional bed utilization and adsorption capacity at breakthrough time. Besides, zeolites with high basicity did not reach the equilibrium capacity due to the low diffusivity of BT into the micropores. Thermogravimetric analyses of the spent adsorbents showed a stronger BT adsorption onto the more basic zeolites. As main conclusion, adsorbents with medium basicity could present the best performance in fuel desulphurization due to their high affinity with sulphur compounds, although diffusion problems should be taken into account.

Keywords Benzothiophene · LSX zeolites · Basicity · Agglomeration · Desulphurization · Adsorption · Fixed bed

Abbreviations

BT	Benzothiophene
C	Sulphur concentration, ppmw
FAU	Faujasite
FBU	Fractional bed utilization; defined as $q_{\mathrm{br}}/q_{\mathrm{sat}}$
K	Equilibrium constant, ppm^{-1}; parameter defined in (2)
q	Adsorption capacity, mg g^{-1}
$q_{\mathrm{D.eq}}$	Adsorption capacity from the isotherm at a given concentration, mg g^{-1}
$q_{\max}$	Maximum adsorption capacity, mg g^{-1}; parameter defined in (2)
S	Sanderson electronegativity of an element; parameter defined in (1)
S_{int}	Sanderson intermediate electronegativity; parameter defined in (1)
t	Time, min
T	Temperature, K

Subscripts and superscripts

0	Initial
br	Breakthrough time
eq	Equilibrium
p, q, r	Stoichiometric coefficient of the atom in a unit cell of adsorbent
P, Q, R	Elements present in zeolite composition
sat	Saturation time

1 Introduction

At present, European legislation limits sulphur content in road fuels to 50 ppmw. This will be reduced to 10 ppmw by 2009 (European Directive 2003/17/CE). However, sulphur concentrations below 1 ppmw have to be achieved for the

---

J.L. Sotelo (✉) · M.A. Uguina · V.I. Águeda
Department of Chemical Engineering, Universidad Complutense de Madrid, 28040 Madrid, Spain
e-mail: jose.sotelo@quim.ucm.es

application of transportation fuels in fuel cells technologies because sulphur would poison the catalysts involved in the process (Hernández-Maldonado and Yang 2004a).

Hydrodesulphurization (HDS) processes are extensively used to remove sulphur from fuels. Higher temperatures, partial pressures of hydrogen, and residence times or more active HDS catalysts are required to achieve the new specifications (Vasudevan and Fierro 1996).

Among all novel technologies described for deep fuel desulphurization, adsorption appears as a soft technology for sulphur removal because hydrogen is not extensively required and mild operation conditions can be used. Several adsorption processes such as IRVAD or Phillips S-Zorb have been developed and industrially proven in order to complement or substitute HDS in refineries (Babich and Moulijn 2003).

The major challenge in adsorption processes is to design an adsorbent that presents a very good performance in dynamic experiments with a high selectivity towards sulphur compounds in presence of other adsorptives. Various types of adsorbents have been used in desulphurization processes, for instance, mixed metal oxides, activated carbon, hydrotalcites, zeolites, aluminophosphates and some novel mesoporous materials (Kim et al. 2006; Salem and Hamid 1997; Nemeth et al. 1994; McKinley and Angelici 2003; Sotelo et al. 2005). π complexation adsorbents based on Y zeolite exchanged with Cu (I) and Ag have been developed by Yang and coworkers and used as selective adsorbents in gas oil desulphurization (Hernández-Maldonado et al. 2004b).

Basic microporous zeolites, e.g. X and Y, have been widely studied for selective adsorption of polar or polarizable molecules, such as sulphur containing compounds from petroleum fractions, due to their tuneable selectivity regarding polar molecules (Davis 1991; Salem and Hamid 1997; Zinnen 1999; Sotelo et al. 2001, 2002).

Cations in zeolites are adsorption sites for molecules with π electrons giving rise to a specific interaction, because of their Lewis acid character, which runs in parallel to cation electronegativity. Basic oxygen atoms in 12R windows are also adsorption sites, which may result from an interaction of CH groups of the aromatic ring with six basic oxygen atoms of the window (Barthomeuf 1996).

The basic character of the zeolites can be analysed by several characterization techniques (Barthomeuf 1996) and also with different parameters (Sanderson 1976; Mortier 1978) in order to predict their selectivity in adsorption experiments (Sun 1994) or their catalytic performance. In this contribution, the Sanderson's intermediate electronegativity of the adsorbents (S_{int}) was calculated as a representative parameter of the adsorbent basicity using the following equation:

$$S_{\mathrm{int}} = (S_P^p \cdot S_Q^q \cdot S_R^r)^{1/(p+q+r)} \qquad (1)$$

where S_I is the Sanderson's electronegativity of the atom I, and p, q and r are the stoichiometric coefficient of the atom I in a unit cell of the adsorbent (Barthomeuf 1996).

This model does not take into account the influence of the adsorbent structure; however, it is very useful to compare zeolites with the same structure because Sanderson's intermediate electronegativity only depends on the chemical composition, presenting lower values for more basic adsorbents.

Equilibrium isotherms are very important for the design of adsorption processes. The shape of an isotherm provides significant information on the adsorption process (Giles et al. 1960). The nature and the strength of the interaction between adsorbate and adsorbent are related to the affinity parameter calculated from the isotherm models (Ma and Yang 2007).

Most adsorbents are synthesised in powder form and must be agglomerated before their use in industrial fixed bed adsorbers in order to reduce the pressure drop.

In this work, the adsorption of benzothiophene (BT) as a model sulphur compound present in road fuels onto agglomerated zeolites with FAU structure has been studied. Several adsorbents with different Si/Al and exchanged with alkaline cations were prepared and agglomerated. Equilibrium experiments were carried out and the data were afterwards fitted to the Langmuir's model. The affinity parameter was related to the Sanderson's intermediate electronegativity as an index of the adsorbent basicity. Kinetic experiments were carried out in order to understand the adsorption mechanism of BT onto basic zeolites. Finally, thermogravimetric experiments were carried out to relate BT desorption temperature to the affinities previously calculated.

2 Experimental

2.1 Adsorbent preparation

Several adsorbents based on zeolites with FAU structure with different Si/Al molar ratio were used. Commercial NaY and NaX zeolites were obtained from Grace Davison and Aldrich respectively. Low silica X zeolite (LSX) was synthesised in the laboratory according to Kühl (Kühl 1987) and exchanged three times with sodium chloride solutions to obtain the NaLSX sample, following the procedure described elsewhere (Sotelo et al. 2001). In the same way, potassium and caesium exchanged zeolites were prepared from the NaLSX zeolite by using the conditions summarised in Table 1.

Powder zeolites were agglomerated with sodium bentonite (5/1, w/w) by preparing a homogeneous suspension of both materials in cyclohexane. Under continuous agitation, water was atomised in the suspension and the resulting product was stirred slowly overnight. The suspension was then

Table 1 Ion exchange conditions and nomenclature of synthesised adsorbents

Powder material	N. of exchanges	Concentration (molar)	Cation	Agglomerated
NaY	–	–		A-NaY
NaX	–	–		A-NaX
LSX	–	–		A-LSX
NaLSX	3	0.5	Na^+	A-NaLSX
KLSX-01	1	0.125	K^+	A-KLSX-01
KLSX-02	1	0.25	K^+	A-KLSX-02
KLSX-05	1	0.5	K^+	A-KLSX-05
KLSX	2	0.5	K^+	A-KLSX
CsLSX-05	1	0.5	Cs^+	A-CsLSX-05
CsLSX	2	0.5	Cs^+	A-CsLSX

filtered, dried at 323 K and calcined at 723 K for four hours. Finally, the agglomerated zeolites were sieved to obtain particles seized in the range 0.177–0.5 mm. The agglomerated samples have been identified by an A before the acronym.

2.2 Characterization of the adsorbent

The BET surface area was calculated from nitrogen adsorption-desorption measurements at 77 K using a Micromeritics Asap-2010 instrument. X-ray diffraction (XRD) patterns were performed on a Philips diffractometer (X'pert MPD) with CuKα radiation and Ni filter. Chemical composition was determined by X-ray fluorescence (XRF) in a Philips PW-1480 instrument. Particle density was determined by Hg porosimetry.

Thermogravimetric analyses (TGA) of spent adsorbents were performed on a thermobalance Exstar 6000 of Seiko Instruments Inc. with a TG/DTA 6200 module under a He flow of 30 $cm^3\,min^{-1}$ and a heating rate of 10 $K\,min^{-1}$ up to 973 K.

2.3 Adsorption experiments

Equilibrium adsorption experiments were carried out in closed Pyrex tubes placed in a thermostatic bath. The initial mixture was prepared with BT (Aldrich) in anhydrous cyclohexane (Merck). 5 g of this mixture were stirred with different weights of adsorbent at 298 K during 2 days. After adsorption, the adsorbents were recovered by centrifugation and dried at 298 K before TGA. BT concentration was measured by gas chromatography (GC) by using a capillary column CPSil5CB.

Dynamic adsorption runs were carried out in a stainless steel downflow fixed bed adsorber, with an internal diameter of 4.9 mm and 0.5 m length, placed in an oven and packed with 3 g of adsorbent (bed length ca. 0.3 m). The temperature of the bed was controlled at 298 K. A displacement pump was used to feed the adsorption mixture into the bed at a constant flow rate of 5 $mL\,min^{-1}$. In all cases, initial mixtures were prepared with BT as model sulphur compound dissolved in cyclohexane with a sulphur content of ca. 250 ppmw. The effluent was analysed by GC.

3 Results and discussion

3.1 Adsorbents properties

All the synthesised zeolites with an average particle diameter of ca. 7 µm were agglomerated with bentonite to obtain particles sized in the range 0.177–0.5 mm.

The SEM images of the adsorbent synthesised (LSX) and agglomerated (A-LSX) are shown in Fig. 1 as a representative sample of the materials.

The powder XRD patterns of the adsorbent synthesised (LSX) and agglomerated (A-LSX) are shown in Fig 2. In all cases the XRD patterns showed FAU structure with lower intensity peaks for the agglomerated samples due to the bentonite dilution effect.

The nitrogen adsorption-desorption isotherms of the LSX and A-LSX samples are shown in Fig. 3. Both materials presented a type I isotherm, with a lower N_2 adsorption capacity for the agglomerated sample because of the bentonite dilution effect. A-LSX sample showed a hysteresis loop at high partial pressures due to the meso-macropores generated during the agglomeration process. The surface areas of LSX and A-LSX samples are 756 and 436 $m^2\,g^{-1}$ respectively. There is a loss of ca. 40% in the surface areas of all samples during the agglomeration process although the proportion of bentonite is only a 17%, which indicates a certain blockage of pores during the agglomeration process.

The physico-chemical properties of the synthesised materials are summarised in Table 2. The composition and Sanderson's intermediate electronegativity refer to the powder synthesised zeolites, whereas the specific surface area and the particle density have been measured for the agglomerated samples.

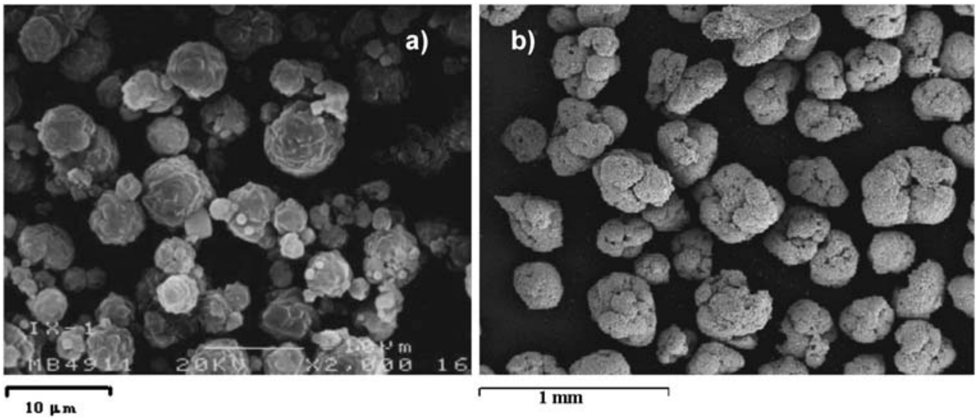

Fig. 1 SEM micrographs of the synthesized materials. (**a**) LSX Zeolite crystals, (**b**) agglomerated particles

Table 2 Physico-chemical properties of the synthesised adsorbents

Adsorbent	Powder material					Agglomerated adsorbent		
	Si/Al (molar)	Na/($\sum$cat) (molar)	K/($\sum$cat) (molar)	Cs/($\sum$cat) (molar)	S_{int}	Surface area ($m^2\,g^{-1}$)	Particle density ($g\,cm^{-3}$)	Micropore volume ($cm^3\,g^{-1}$)
A-NaY	2.85	1	–	–	2.623	446	0.562	0.196
A-NaX	1.27	1	–	–	2.391	592	0.836	0.251
A-NaLSX	1.07	0.95	0.05	–	2.320	452	0.884	0.233
A-LSX	1.07	0.75	0.25	–	2.308	436	0.870	0.204
A-KLSX-01	1.07	0.70	0.30	–	2.304	444	0.958	0.215
A-KLSX-02	1.07	0.60	0.40	–	2.296	449	0.942	0.214
A-KLSX-05	1.07	0.50	0.50	–	2.289	490	0,978	0.190
A-KLSX	1.07	0.35	0.65	–	2.271	424	0.974	0.194
A-CsLSX-05	1.07	0.52	–	0.48	2.171	345	1.448	0.158
A-CsLSX	1.07	0.45	–	0.55	2.159	317	1.033	0.142

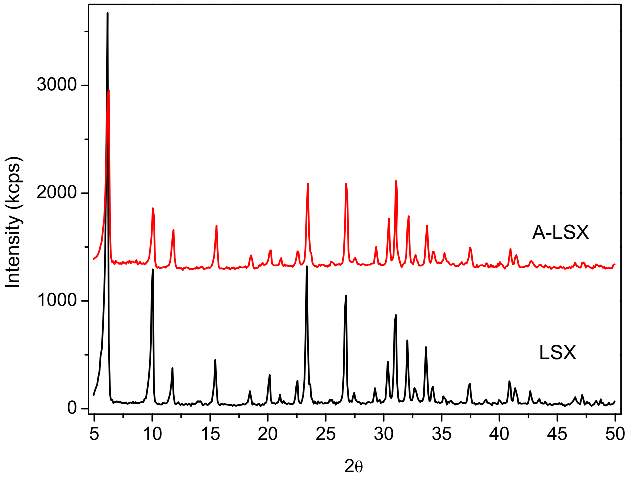

Fig. 2 XRD patterns of the synthesised materials

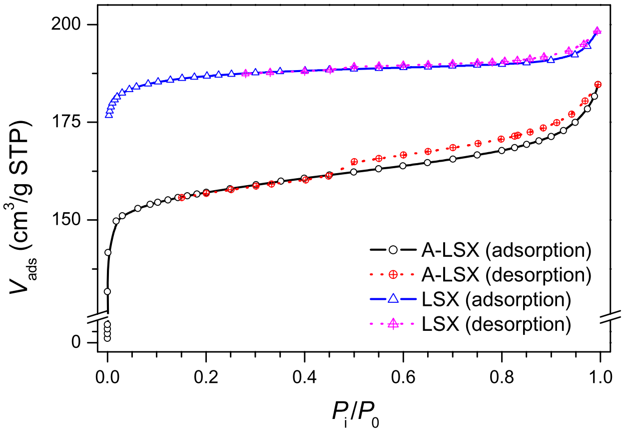

Fig. 3 N_2 adsorption-desorption isotherms at 77 K of the synthesised materials

Table 2 shows that incomplete ion exchange was achieved, being the maximum value (% molar): 95, 65 and 55 for Na-LSX, KLSX and CsLSX, respectively. Logically the maximum value reached is related to the size of the exchanged cation: Na<K<Cs. BET surface area of the alkali-exchanged agglomerated zeolites was lower than that of the corresponding commercial samples (A-NaY and A-NaX), and decreased with the exchanged cation size: A-

NaLSX > A-KLSX ≫ A-CsLSX. Particle density increased as the atomic weight of the exchanged cations rose.

As expected, S_{int} values indicate that basicity increases as the Si/Al molar ratio and the cation electronegativity decrease (Mortier 1978; Barthomeuf 1996), being CsLSX the adsorbent with higher basicity (lower S_{int} value).

3.2 Adsorption experiments

Benzothiophene is a slightly polar molecule due to the presence of a sulphur atom in their molecular structure. The charge distribution has been estimated by molecular modelling (Accelrys ViewerPro 4.2 Preview®). Calculations showed a negative charge density onto the sulphur atom (−0.097 A.U.). More polar molecules such as indole (−0.256 A.U.) are adsorbed stronger than BT onto these zeolites (Sotelo et al. 2002), which confirms a high influence of molecular polarity on zeolite adsorption performance.

In order to analyse the adsorption performance of FAU zeolites in the desulphurization process, the adsorption capacities of several agglomerated basic zeolites at different equilibrium concentrations of benzothiophene in the liquid phase were determined.

3.2.1 Influence of the Si/Al molar ratio

BT adsorption isotherms onto several adsorbents are shown in Fig. 4. All the adsorbents present a type I isotherm, characteristic of adsorption processes onto microporous materials. Experimental data have been fitted to the Langmuir adsorption isotherm:

$$q = \frac{q_{\max} \cdot K \cdot C_{\text{eq}}}{1 + K \cdot C_{\text{eq}}} \qquad (2)$$

where, q is the adsorption capacity at a given equilibrium concentration (C_{eq}), $q_{\max}$ is the maximum adsorption capacity and K is the adsorption equilibrium constant. These parameters were obtained and listed in Table 3.

The maximum adsorption capacity is usually related to the pore volume and BET surface areas. In this case, A-NaLSX adsorbent presents a medium pore volume and surface area as compared with A-NaY and A-NaX (Table 2), although it shows the lowest maximum adsorption capacity ($q_{\max}$). This could be due to a possible blocking of the pore windows with strongly adsorbed BT molecules that hinder the adsorption of other BT molecules into the inner pores, because of the higher polarity of this zeolite. The adsorption equilibrium constant values are related to the basicity of the material, the highest K value was obtained for A-NaLSX zeolite, which has the lowest Si/Al molar ratio and therefore the highest basicity.

Breakthrough curves of BT over different adsorbents are shown in Fig. 5. Adsorption capacities at saturation time, q_{sat}, and at breakthrough time, q_{br}, as well as the fractional bed utilization, *FBU*, defined as the ratio $q_{\text{br}}/q_{\text{sat}}$ have been obtained. These are listed in Table 4, which includes the adsorption capacity deduced from the isotherm ($q_{\text{D.eq}}$).

As revealed by Fig. 5, the diffusion into the micropores is more important at lower relative times for A-NaLSX, followed by A-NaX and A-NaY. As all these materials have the same pore size, the variation in the performance can be

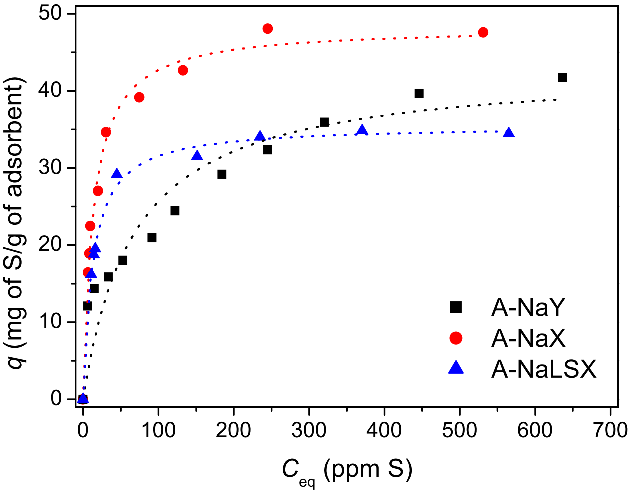

Fig. 4 BT adsorption isotherms onto materials synthesised with different Si/Al. *Dotted lines*: calculated values from Langmuir isotherm

Table 3 Parameters obtained from Langmuir isotherms. Si/Al molar ratio influence

Adsorbent	$q_{\max}$ (mg g^{-1})	K (ppm^{-1})	r^2
A-NaY	44.1 ± 3.6	0.015 ± 0.004	0.903
A-NaX	48.3 ± 1.0	0.076 ± 0.006	0.991
A-NaLSX	35.5 ± 0.5	0.079 ± 0.005	0.996

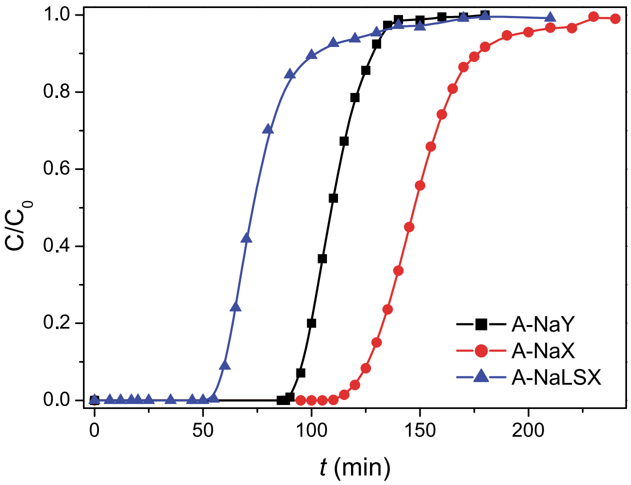

Fig. 5 BT breakthrough curves onto materials with different Si/Al

Table 4 Parameters obtained from the breakthrough curve

Adsorbent	C_0 (ppm S)	$q_{\mathrm{D.eq}}$ (mg g^{-1})	q_{br} (mg g^{-1})	q_{sat} (mg g^{-1})	*FBU*
A-NaY	256	34.1	28.1	35.4	0.80
A-NaX	252	45.9	34.5	47.8	0.72
A-NaLSX	260	34.0	17.1	25.4	0.67

Table 5 Parameters obtained from Langmuir isotherms. Exchange cation influence

Adsorbent	$q_{\max}$ (mg g^{-1})	K (ppm^{-1})	r^2
A-NaLSX	35.5 ± 0.5	0.079 ± 0.005	0.996
A-LSX	39.3 ± 2.4	0.208 ± 0.045	0.938
A-KLSX-01	33.4 ± 1.2	0.514 ± 0.084	0.946
A-KLSX-02	35.7 ± 0.6	0.928 ± 0.080	0.988
A-KLSX-05	26.7 ± 1.2	0.465 ± 0.115	0.925
A-KLSX	28.6 ± 3.2	0.226 ± 0.132	0.442
A-CsLSX-05	31.2 ± 0.4	0.034 ± 0.018	0.996
A-CsLSX	27.8 ± 0.5	0.033 ± 0.002	0.986

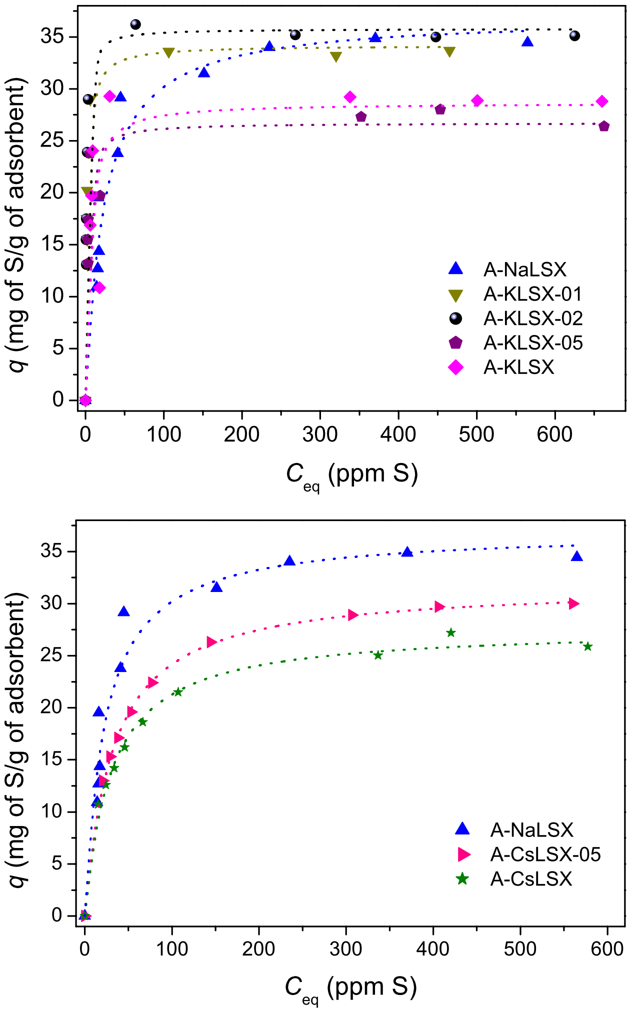

Fig. 6 BT adsorption isotherms onto materials exchanged with different cations. *Dotted lines*: calculated values from Langmuir isotherm

explained taking into account the different adsorbate affinity with the adsorbent surface.

The saturation and the breakthrough time capacities follow the trend observed in the equilibrium isotherms, A-NaX > A-NaY > A-NaLSX. The adsorption capacities at saturation time are similar to equilibrium capacities at the same concentration for A-NaY and A-NaX; however, A-NaLSX sample showed lower saturation capacity than the equilibrium one. This fact can be explained by considering that A-NaLSX zeolite, with a lower Si/Al molar ratio, has a higher polarity and therefore adsorbs BT more strongly than the other materials, hindering the adsorption of other BT molecules into the pores.

3.2.2 *Influence of the exchanged cation*

Adsorption isotherms of BT onto exchanged LSX zeolites are shown in Fig. 6. All the adsorbents present a type I isotherm, being the experimental data fitted to the Langmuir model, with their parameters listed in Table 5.

The maximum adsorption capacity decreases with the cation electronegativity, i.e. with the higher basic character of the adsorbent. This result can be explained by considering that the lowest electronegative cation (Cs) presents the highest ionic radius and therefore a zeolite exchanged with this cation usually presents a lower micropore volume.

The affinity parameter calculated, K, shows the higher values for potassium exchanged zeolites. This trend can be explained by considering two different adsorption mechanisms onto these adsorbents, which are sketched in Fig. 7.

The first mechanism (Fig. 7a) is the interaction of the π electron cloud of the BT molecule with the cations, which is higher for cations with high electronic affinity such as sodium. The second one (Fig. 7b) is the interaction of the hydrogen atoms which are in a BT molecule with the basic oxygen atoms of the zeolite framework (Barthomeuf 1996); the oxygen charge density and therefore their interaction with H atoms is higher for adsorbents exchanged with caesium. In other words, as the cation electronegativity is lower, its charge density and the interaction with the π electron cloud decrease, although the basic character of the adsorbent is enhanced, since the interaction of basic oxygen with hydrogen atoms is stronger. In this case, BT seems to be

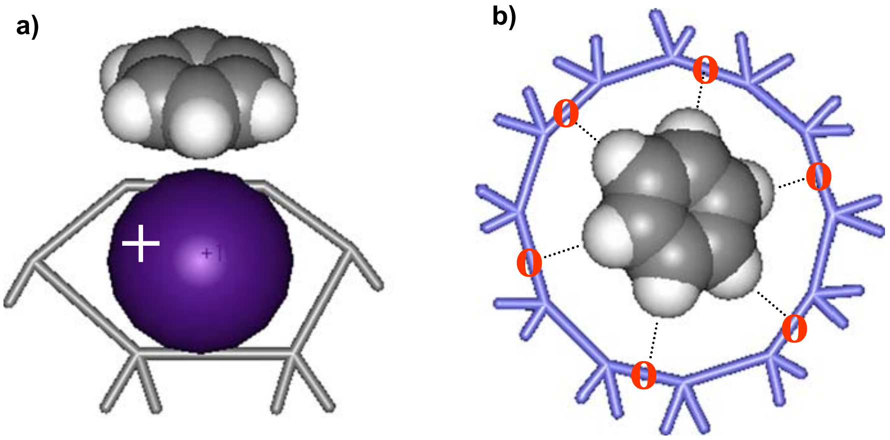

Fig. 7 Adsorption mechanisms onto zeolites with FAU structure: (**a**) molecule interaction with the cation, (**b**) molecule interaction with basic oxygens

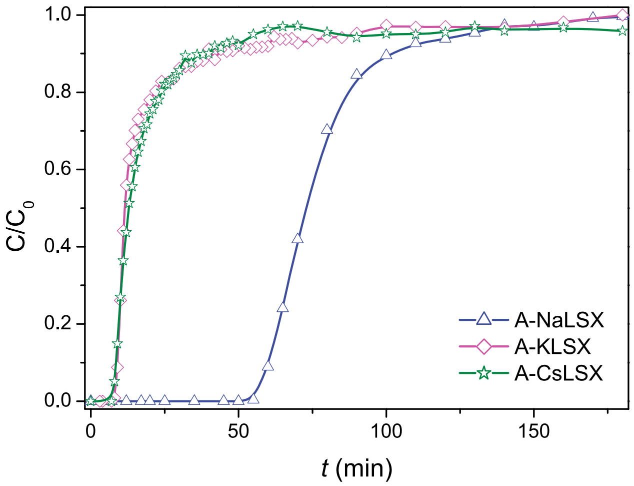

Fig. 8 BT breakthrough curves onto materials with different exchange cation

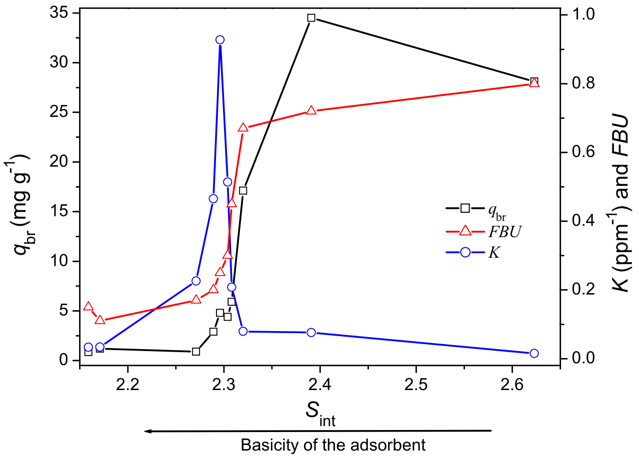

Fig. 9 Basicity influence on adsorption parameters

adsorbed more strongly onto adsorbents where both adsorption mechanisms have a high influence, i.e. adsorbents with medium basicity.

The most significant BT breakthrough curves onto exchanged adsorbents are shown in Fig. 8, and the adsorption parameters calculated for all the agglomerated adsorbents are listed in Table 6. It is shown that very long times are required to reach saturation due to the very low diffusivity of BT into the micropores.

The adsorption capacity at saturation and breakthrough times, and also the *FBU* decrease as the basicity of the adsorbent increases. It is worth noting that the adsorption capacities at saturation time of the adsorbents exchanged with potassium and caesium are much lower than those obtained from the isotherm at a given concentration. These two facts can be explained by recognising that BT is strongly adsorbed onto these adsorbents, and then, the higher the interaction with the active sites, the slower the diffusion of BT molecules into the micropores; in other words, BT molecules adsorbed on the pore windows hinder the diffusion and the adsorption of other BT molecules into the micropores. The adsorption mechanism of BT in dynamic experiments starts with the diffusion into the macropores, is followed by the adsorption onto the pore windows and is completed with the slow diffusion into the micropores (Uguina et al. 2005).

A summary of the adsorption parameters related to basicity of the adsorbent is shown in Fig. 9. As revealed by the figure, an increase in the adsorbent basicity (lower values of S_{int}) leads to a decrease in both the *FBU* and the q_{br}; therefore, few basic adsorbents might be appropriate in desulphurization processes; however, when competitive adsorptives are present in commercial fuels, and adsorbents with high affinities are required (Sotelo et al. 2001, 2002). So, there are two different considerations in order to select the adsorbent for desulphurization processes: the dynamic performance, and the selectivity to sulphur compounds in presence of competitive adsorptives. From our results medium basicity adsorbents could be the more appropriate.

Table 6 Parameters obtained from the breakthrough curve

Adsorbent	C_0 (ppm S)	$q_{\mathrm{D.eq}}$ (mg g^{-1})	q_{br} (mg g^{-1})	q_{sat} (mg g^{-1})	*FBU*
A-NaLSX	260	34.0	17.1	25.4	0.67
A-LSX	250	38.4	5.9	13.1	0.45
A-KLSX-01	249	33.3	4.4	14.9	0.30
A-KLSX-02	250	35.5	4.8	19.1	0.25
A-KLSX-05	262	26.3	2.9	14.6	0.20
A-KLSX	257	28.0	0.9	5.2	0.17
A-CsLSX-05	241	27.8	1.2	11.0	0.11
A-CsLSX	246	24.7	0.86	5.7	0.15

3.3 Regeneration of adsorbents

The enthalpy of adsorption is related to the temperature of desorption (Delgado and Gómez 2005), i.e. the higher the temperature of desorption, the higher the interaction between the adsorbate and the adsorbent surface. To show the influence of the Si/Al molar ratio and the exchanged cation on the thermal regeneration of adsorbents, TG analyses have been performed on the spent adsorbents after the dynamic adsorption experiments. The area of desorption peaks can be related to the amount of adsorbate desorbed at different temperatures.

3.3.1 Influence of the Si/Al molar ratio

TGA plots of the recovered adsorbents (Fig. 10) show a first weight loss at temperatures lower than 523 K that corresponds to solvent, water and weakly adsorbed BT (the presence of BT in the first peak was checked by MS coupled with TG). A second peak appears at temperatures higher than 523 K due to the fact that BT is strongly adsorbed; its area decreases with the adsorbent Si/Al ratio, according to the higher adsorbent-BT interaction previously discussed.

Finally, as the Si/Al molar ratio of the adsorbent decreases, a third desorption peak at temperatures higher than 773 K appeared. This fact could be explained by considering BT interactions on various active sites as the aluminium content of the FAU structure increases. This result agrees with the high affinities calculated for those materials. NaLSX, due to its lower Si/Al molar ratio, presents both a higher amount of adsorption sites and the highest interaction with the BT molecule. So, BT would be more strongly adsorbed on X zeolites which have more adsorption sites than Y zeolites.

3.3.2 Influence of the exchange cation

Figure 11 shows the TGA plots of recovered adsorbents with Si/Al = 1 exchanged with different alkaline cations. All adsorbents presented quite similar TG profiles and BT desorption temperatures.

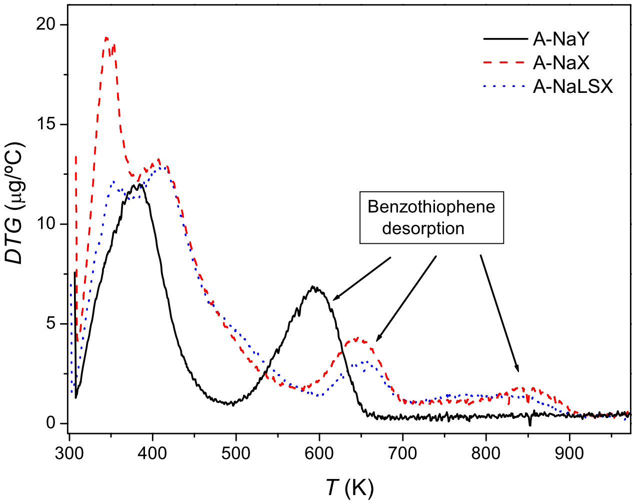

Fig. 10 TGA of spent samples synthesised with different Si/Al

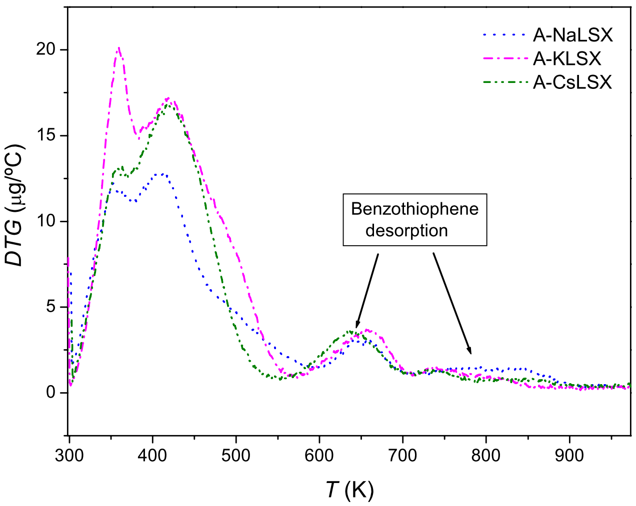

Fig. 11 TGA of spent samples exchanged with different cations

A-KLSX and A-CsLSX show a very small peak at temperatures higher than 773 K due to the low saturation capacities of these adsorbents in dynamic experiments. However, these peaks appeared at temperatures close to the NaLSX ones because the adsorption centres are quite similar. From the breakthrough curves of BT onto these adsorbents and the TGA runs, it can be concluded that A-KLSX and A-CsLSX present a very high interaction with BT molecules. Despite of the very low adsorption capacities at saturation time, these materials would give better results in presence of other competitive adsorptives.

4 Conclusions

The basicity of the adsorbent increased as the Si/Al and the cation electronegativity decreased. The affinity coefficient reaches the highest values for potassium exchanged LSX zeolites, that is to say medium to high basic adsorbents have to be used to get high selectivity towards sulphur compounds. Adsorption capacities at breakthrough time and the fractional bed utilisation decreased with the basicity, in other words, less basic adsorbents presented better performances in dynamic experiments. However, dynamic experiments showed that the adsorption capacity at saturation time was much lower than those expected from the isotherm for highly basic adsorbents. Therefore, the affinity and the diffusivity have to be considered in order to select an adsorbent for desulphurization. Regeneration experiments showed high BT desorption temperatures that increased as the basicity of the adsorbent rose.

Acknowledgements Financial support from E.U. and Comunidad Autónoma de Madrid through the projects FEDER European Project 2FD1997-1873 and CAM 07M/0056/2001 is gratefully acknowledged.

References

European Union Parliament and Council: Directive 2003/17/CE of the European Parliament and Council of the 3 March 2003 concerning the quality of petrol and diesel fuel. Off. J. Eur. Commun. **L76**, 10–19 (2003)

Babich, I.V., Moulijn, J.A.: Science and technology of novel processes for deep desulfurization of oil refinery streams: a review. Fuel **82**, 607–631 (2003)

Barthomeuf, D.: Basic zeolites characterization and uses. Catal. Rev. **38**, 521–612 (1996)

Davis, M.E.: Zeolites and molecular sieves: not just ordinary catalysts. Ind. Eng. Chem. Res. **30**, 1675–1683 (1991)

Delgado, J.A., Gómez, J.M.: Modelling of temperature-programmed desorption thermograms for the determination of adsorption heat considering pore and surface diffusion. Langmuir **21**(8), 3503–3510 (2005)

Giles, C.H., MacEwan, T.H., Nakhwa, S.N., Smith, D.: Studies in adsorption. Part XI*. A system of classification of solution adsorption isotherms, and its use in diagnosis of adsorption mechanisms and in measurement of specific surface areas of solids. J. Chem. Soc., 3973–3993 (1960)

Hernández-Maldonado, A.J., Yang, R.T.: New sorbents for desulfurization of diesel fuels via π-complexation. AIChE J. **50**, 791–801 (2004a)

Hernández-Maldonado, A.J., Stamatis, S.D., Yang, R.T., He, H.Z., Cannella, W.: New layered sorbents for desulfurization of diesel fuels via π-complexation: layered beds and regeneration. Ind. Eng. Chem. Res. **43**, 769–776 (2004b)

Kim, J.H., Ma, X.L., Zhou, A.N., Song, C.S.: Ultra-deep desulfurization and denitrogenation of diesel fuel by selective adsorption over three different adsorbents: a study on adsorptive selectivity and mechanism. Catal. Today **111**, 74–83 (2006)

Kühl, G.H.: Crystallization of low-silica faujasite ($SiO_2/Al_2O_3 \approx 2.0$). Zeolites **7**, 451–457 (1987)

Ma, L., Yang, R.T.: Selective adsorption of sulfur compounds: Isotherms, heats, and relationship between adsorption from vapor and liquid solution. Ind. Eng. Chem. Res. **46**, 2760–2768 (2007)

McKinley, S.G., Angelici, R.J.: Deep desulphurization by selective adsorption of dibenzothiophenes on Ag^+/SBA-15 and Ag^+/SiO_2. Chem. Commun., 2620–2621 (2003)

Mortier, W.J.: Zeolite electronegativity related to physicochemical properties. J. Catal. **55**, 138–145 (1978)

Nemeth, L.T., Kulprathipanja, S., Arena, B.J., Holmgren, J.S.: Removal of sulfur compounds from liquid organic feedstreams. US Patent 5,360,536, 1 Nov 1994

Salem, A.B., Hamid, H.S.: Removal of sulfur compounds from naphta solutions using solid adsorbents. Chem. Eng. Technol. **20**, 342–347 (1997)

Sanderson, R.T.: Chemical Bonds and Bond Energy. Academic Press, New York (1976)

Sotelo, J.L., Uguina, M.A., Romero, M.D., Gómez, J.M., Águeda, V.I., Ortiz, M.A.: Dibenzothiophene adsorption over zeolites with faujasite structure. Stud. Surf. Sci. Catal. **135**, 227 (2001)

Sotelo, J.L., Uguina, M.A., Águeda, V.I.: Adsorption of indole and benzothiophene over zeolites with faujasite structure. Stud. Surf. Sci. Catal. **142B**, 1579–1586 (2002)

Sotelo, J.L., Uguina, M.A., Águeda, V.I., Serrano, J.: Desulphurization of fuels by liquid adsorption onto mesoporous materials. Stud. Surf. Sci. Catal. **158B**, 1089–1098 (2005)

Sun, D.-M.: Dependence of X zeolite adsorption properties on electronegativity and vibration frequency. Vacuum **45**, 1175–1179 (1994)

Uguina, M.A., Sotelo, J.L., Delgado, J.A., Gómez, J.M., Celemín, L.I.: Adsorption of methyl ethyl ketone and trichloroethene from aqueous solutions onto silicalite fixed-bed adsorbers. Sep. Purif. Technol. **42**, 91–99 (2005)

Vasudevan, P.T., Fierro, J.L.G.: A review of deep hydrodesulfurization catalysis. Catal. Rev. Sci. Eng. **38**, 161–188 (1996)

Zinnen, H.A.: Removal of organic sulfur compounds from FCC gasoline using regenerable adsorbents. US Patent 5,935,422, 10 Aug 1999